(Dumont, J., & Nunez, J., Eds.) pp 31–48, Elsevier/North-Holland Biomedical Press, Amsterdam.
Swaneck, G. E., Nordstrom, J. L., Kreuzaler, F., Tsai, M. J., & O'Malley, B. W. (1979) *Proc. Natl. Acad. Sci. U.S.A. 76*, 1049–1053.
Taylor, R. N., Swaneck, G. E., & Smith, R. G. (1980) *Biochem. J. 192*, 385–393.
Tsai, M. J., Ting, A. C ., Nordstrom, J. L., Zimmer, W., & O'Malley, B. W. (1980) *Cell (Cambridge, Mass.) 22*, 219–230.

The Glu(B13) Carboxylates of the Insulin Hexamer Form a Cage for Cd^{2+} and Ca^{2+} Ions†

Michael C. Storm‡ and Michael F. Dunn*
Department of Biochemistry, University of California, Riverside, California 92521
Received August 6, 1984

ABSTRACT: Substitution of Cd^{2+} for Zn^{2+} yields a hexameric insulin species containing 3 mol of metal ion per hexamer. The Cd^{2+} binding loci consist of the two His(B10) sites and a new site involving the Glu(B13) residues located at the center of the hexamer [Sudmeier, J. L., Bell, S. J., Storm, M. C., & Dunn, M. F. (1981) *Science (Washington, D.C.) 212*, 560–562]. Substitution of Co^{2+} or Co^{3+} for Zn^{2+} gives hexamers containing 2 mol of metal per hexamer. Insulin solutions to which both Cd^{2+} and Co^{2+} have been added in a ratio of 6:2:1 [In]:[Co^{2+}]:[Cd^{2+}] followed by oxidation to the exchange-inert Co^{3+} state yield stable hybrid species containing both Co^{3+} and Cd^{2+} with a composition of $(In)_6(Co^{3+})_2Cd^{2+}$. The kinetics of the reaction of 2,2′,2″-terpyridine (terpy) with the exchange-labile $(In)_6(Cd^{2+})_2$ and $(In)_6(Co^{2+})_2$ derivatives are biphasic and involve the rapid formation of an intermediate with coordination of one terpy molecule to each protein-bound metal ion; then, in a rate-limiting step the terpy-coordinated metal ion dissociates from the protein, and a second molecule of terpy binds to the metal ion to form a bis complex. Reaction of the exchange-inert Co^{3+} ions of $(In)_6(Co^{3+})_2$ with terpy is a slow apparent first-order process ($t_{1/2}$ = 13.1 h). In contrast to the kinetic behavior of $(In)_6(Co^{2+})_2$ and $(In)_6(Cd^{2+})_2$, the Cd^{2+} ions bound to the hybrid $(In)_6(Co^{3+})_2Cd^{2+}$ react quite slowly with terpy ($t_{1/2}$ = 1 h at pH 8.0). We postulate that Cd^{2+} is caged within the central cavity of this hybrid hexamer at the Glu(B13) site and that the rate of reaction with terpy is determined by the slow rate of escape of Cd^{2+} from this cage. Competition studies indicate that Ca^{2+} and Cd^{2+} compete for the Glu(B13) site. Equilibrium binding studies using $^{45}Ca^{2+}$ substantiate the presence of a single high-affinity calcium binding site with k_D = 83 μM, which we propose involves the Glu(B13) carboxylates.

The elegant X-ray crystallographic work of Hodgkins, Dodson, and their co-workers [see Blundell et al. (1972) and Emdin et al. (1980)] has shown the zinc–insulin hexamer $(In)_6(Zn^{2+})_2$[1] to be a torus-shaped molecule (Chart I) with the two zinc ions separated by 17 Å and located on the 3-fold symmetry axis in a solvent-filled cavity that runs through the hexamer. The two zincs reside in octahedral ligand fields each coordinated by three histidyl imidazolyl groups [the His(B10) residues] and by three water molecules.

Previous work from this laboratory (Dunn et al., 1980) has shown that, in agreement with earlier literature (Fredericq, 1954; Tanford & Epstein, 1974a,b; Brill & Venable, 1967, 1968), the two high-affinity zinc sites observed in solution have kinetic and thermodynamic properties consistent with assignment of these sites to the crystallographically identified His(B10) sites. Our kinetic and thermodynamic evidence indicate that the assembly of the $(In)_6(Zn^{2+})_2$ species is a highly cooperative process (Dunn et al., 1980). Fourier-transform ^{113}Cd NMR experiments with $^{113}Cd^{2+}$-substituted insulin (Sudmeier et al., 1981) led to the discovery that, in concentrated solutions, Cd^{2+} substitution for Zn^{2+} results in the formation of a cadmium–insulin species presumed to be $(In)_6(Cd^{2+})_2Cd^{2+}$. The two classes of high-affinity Cd^{2+} sites were identified as (1) the two His(B10) sites and (2) a new site proposed to involve the Glu(B13) carboxylates located at the center of the hexamer (viz., Chart I). Metal ion substitution experiments with the $^{113}Cd^{2+}$-substituted species indicated that both $(In)_6(Cd^{2+})_2$ and $(In)_6(Zn^{2+})_2$ are calcium binding proteins and that Ca^{2+} can displace Cd^{2+} from the Glu(B13) site but not from the His(B10) sites (Sudmeier et al., 1981).

Crystallographic studies (Blundell et al., 1972; Emdin et al., 1980) also indicate the Glu(B13) residues form metal ion binding sites. In their review, Blundell et al. (1972) make brief mention of a $(In)_6(Cd^{2+})_2Cd^{2+}$ hexamer with cadmium bound both to the His(B10) sites and to the Glu(B13) site. Emdin

†This work was supported by grants from the National Science Foundation, the American Diabetes Association, and the National Institutes of Health.
‡Present address: Medical Department, American McGaw, Irvine, CA 92714.

[1] Abbreviations: In or P, insulin; $(In)_6(M^{x+})_m(M^{y+})_n$, metal-coordinated insulin hexamers where x and y designate the metal ion valencies and m and n the stoichiometries of metal ions bound to the His(B10) and Glu(B13) sites, respectively; terpy, 2,2′,2″-terpyridine; Tris, 2-amino-2-(hydroxymethyl)-1,3-propanediol.

0006-2960/85/0424-1749$01.50/0

Chart I: Three-Dimensional Perspective of the Insulin Hexamer Showing Positions and Liganding of Crystallographically Identified His(B10) Zn^{2+} Sites (Site I) and the Proposed Glu(B13) Ca^{2+} Site (Site II)[a]

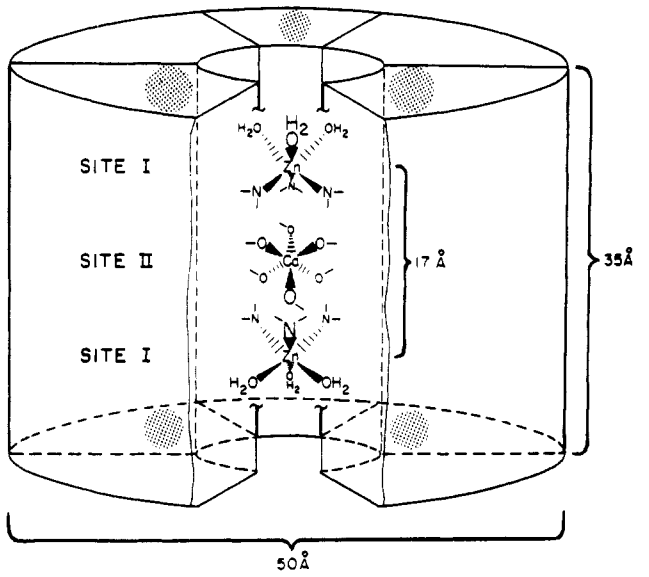

[a] One monomer has been cut away to show the central cavity. The shaded areas indicate the trimer of dimers symmetry of the hexamer [redrawn with permission from Sudmeier et al. (1981)].

et al. (1980) report some of the details of a $(In)_6(Zn^{2+})_2(Zn^{2+})_3$ hexamer containing one zinc each at the two His(B10) sites and one zinc bound to each pair of Glu(B13) residues.

In this work we report some of the physical and chemical properties of Cd^{2+}-, Co^{2+}-, and Co^{3+}-substituted insulin hexamers and of Cd^{2+}–Co^{3+} hybrid hexamers. Evidence is presented that substantiates the discovery that the six Glu(B13) residues within the $(In)_6(Zn^{2+})_2$ hexamer form a cage that binds Ca^{2+} and Cd^{2+}.

Materials and Methods

Materials

Unless otherwise stated, the chemicals employed in these studies were reagent grade or better. Insulin (bovine, crystalline), 2,2′,2″-terpyridine, Tris base, Sephadex G-100, and Sephadex G-25 were purchased from Sigma Chemical Co. Porcine insulin was purchased from Eli Lilly. Chelex 100 (100–200 mesh) was purchased from Bio-Rad. Zn^{2+}, Co^{2+}, and Cd^{2+} (as the certified atomic absorption standards) were purchased from Alfa. Cellulose dialysis tubing was obtained from Union Carbide Corp. Diaflow PM-10 filters were purchased from Amicon Corp. The ^{45}Ca was supplied carrier free by New England Nuclear.

Methods

Metal-free H_2O (pH 8.00) and metal-free 0.05 M Tris–$HClO_4$ buffer, pH 8.00, containing <0.5 μM transition metal ions were prepared by elution over a Chelex 100 column. Metal-free insulin stock solutions containing <0.002 mol of Zn^{2+} per insulin monomer were prepared as previously described (Dunn et al., 1980). The metal ion(s) of choice were added as required just prior to use. Insulin concentrations, expressed as monomers, were determined from the absorbance at 280 nm with a molar extinction coefficient of 5.7×10^3 M^{-1} cm^{-1} (Blundell et al., 1972).

UV–Visible Spectra of Kinetic Studies. UV–visible spectra were collected on a Hewlett-Packard 8450A UV–visible spectrophotometer. Single-wavelength, rapid kinetic measurements and the kinetic analyses were made on a Durrum stopped-flow apparatus and computerized data acquisition system as previously described (Dunn, et al., 1979, 1980).

Quantitation of Metal Content. The metal ion content of solutions was quantitated by atomic absorption spectroscopy or by reaction of a dilute sample with excess terpy (Pattison & Dunn, 1975). The following molar extinction coefficients were used for terpy and terpy–zinc complexes, and all have the units M^{-1} cm^{-1}: terpy, $\epsilon_{290} = 1.60 \times 10^4$; $(terpy)Zn^{2+}$, $\epsilon_{317} = 2.2 \times 10^4$ and $\epsilon_{330} = 2.3 \times 10^4$; $(terpy)_2Zn^{2+}$, $\epsilon_{320} = 3.9 \times 10^4$ and $\epsilon_{333} = 4.1 \times 10^4$ (Holyer et al., 1966). The following molar extinction coefficients (M^{-1} cm^{-1}) for Cd^{2+} and Co^{3+} complexes with terpy were determined: $(terpy)_2Cd^{2+}$, $\epsilon_{332} = 3.32 \times 10^4$; $(terpy)_2Co^{3+}$, $\epsilon_{320} = 2.88 \times 10^4$.

^{45}Ca Binding by Equilibrium Dialysis. Binding of $^{45}Ca^{2+}$ to insulin was studied by using a homemade equilibrium dialysis apparatus via the procedure of Furlong et al. (1972). Equilibrium was achieved by slow rotation of the entire apparatus at 4 °C for at least 12 h. Aliquots were assayed in ACS aqueous scintillation cocktail (Amersham), and the Ca^{2+} concentration was determined by comparison to $^{45}Ca^{2+}$ standards. Another aliquot was used both for protein determination by 280-nm absorbance and for zinc ion determination by reaction with excess terpy.

Amino Acid Analysis. Analyses were performed by the method of Spackman et al. (1958) and Moore & Stein (1963) using an accelerated system (Spackman, 1967) with the Beckman Model 120C amino acid analyzer. Cysteic acid was quantitated on the basis of a standard preparation (Sigma) with and without other standards (Beckman).

Sephadex G-100 Column Chromatography. Sephadex G-100 column chromatography was performed on samples of $^{57}Co^{2+}$-, $^{57}Co^{3+}$-, and Cd^{2+}-substituted insulins as previously described (Dunn et al., 1980). The insulin content of each fraction was determined from the absorbance at 280 nm. The ^{57}Co content of fractions was determined with a Beckman Biogamma II gamma counter. The Cd^{2+} content was determined by atomic absorption spectroscopy and by titration with terpy.

Preparation of the $^{57}Co(III)$ Exchange-Inert Insulin Complex. The ^{57}Co (New England Nuclear) was diluted with isotopically normal Co^{2+} such that the total concentration was 15.3 mM in cobalt and contained 0.05 μCi/mL ^{57}Co. A sample of this ^{57}Co was added to metal-free bovine insulin in metal-free buffer, pH 8.00, to give a Co^{2+} to insulin (monomer) ratio of 0.38. This sample was applied to a G-100 column (2.2 × 56 cm) and eluted with metal-free buffer. The majority of the protein and radioactivity eluted in a single peak at an elution volume characteristic of native insulin hexamer. This material was pooled, and an aliquot of this material, $(In)_6(Co^{2+})_2$, was removed for acid hydrolysis and amino acid analysis (Table I).

Conversion of Co^{2+} to Co^{3+} was achieved by oxidation with H_2O_2 (final concentration 88 mM) at 25 °C for 15 h. The oxidation process was followed both by the increase in absorbance at 525 nm and by the decrease in Co^{2+} titrated by terpy. The oxidized sample contained less than 3% of the original cobalt as Co^{2+}. The sample was concentrated via ultrafiltration, applied to a G-100 column equilibrated with 0.05 M Tris–$HClO_4$ buffer (pH 8.00) containing 0.1 mM H_2O_2, and eluted essentially as a single peak at a volume characteristic of native insulin hexamer. An aliquot of this material, $(In)_6(Co^{3+})_2$, was removed for acid hydrolysis and amino acid analysis (Table I).

Isolation and Identification of a Thermolysin-Generated Peptide Containing $^{57}Co(III)$. The sample of $(In)_6(^{57}Co^{3+})_2$

Table I: Amino Acid Analysis of Co(II)- and Co(III)-Substituted Bovine Insulin Hexamers

	$(In)_6(CO^{2+})_2$		$(In)_6(Co^{3+})_2$		metal-free insulin		
amino acid	yield[a]	residues[b]	yield[a]	residues[b]	yield[a]	residues[b]	insulin expected[c]
Lys	2.9	1.1	5.9	1.0	5.7	1.0	1
His	5.4	2.0	11.9	2.0	11.3	2.0	2
Arg	2.9	1.1	6.6	1.1	4.7	0.8	1
cysteic acid							
Asp	8.4	3.1	19.0	3.2	19.1	3.4	3
Thr	2.5	0.9	5.9	1.0	5.2	0.9	1
Ser	7.5	2.8	17.1	2.9	16.0	2.8	3
Glu	18.6	6.8	45.1	7.5	42.0	7.4	7
Pro	3.0	1.1	7.1	1.2	7.1	1.2	1
Gly	11.0	4.0	25.7	4.3	25.1	4.4	4
Ala	8.4	3.1	19.1	3.2	18.7	3.3	3
$^1/_2$-Cys	13.4	4.9	37.5	6.3	37.0	6.5	6
Val	13.0	4.8	27.3	4.6	27.0	4.8	5
Met							
Ile	1.9	0.7	4.3	0.7	4.3	0.8	1
Leu	15.3	5.7	38.1	6.4	36.3	6.4	6
Tyr	9.8	3.6	22.6	3.8	21.7	3.8	4
Phe	7.5	2.8	18.7	3.1	18.9	3.3	3

[a] Nanomoles. [b] Relative to His as 2. [c] On the basis of the bovine insulin sequence.

was converted to a mixture of A and B chains via performic acid oxidation of the cysteine residues (Hirs, 1967), the ^{57}Co-containing insulin B chains were separated by Sephadex G-25 chromatography, and an aliquot was removed for acid hydrolysis and amino acid analysis (Table II). A second aliquot was hydrolyzed at 37 °C for 4 h with thermolysin (Boehringer Mannheim) at 10% w/w. The hydrolyzed sample was eluted over a Sephadex G-25 column with 50 mM ammonium carbonate buffer containing 0.1 mM H_2O_2. The fractions containing ^{57}Co were pooled and lyophilized, and aliquots were subjected to acid hydrolysis and amino acid analysis (Table II).

N-Terminal Analysis. The N-terminal amino acid of the isolated peptide was determined by a single cycle of the Edman degradation according to the procedure of Lu et al. (1981).

Preparation of the $(In)_6(Co^{3+})_2Cd^{2+}$ Hybrid. Hybrid Co^{3+}–Cd^{2+} hexamers were prepared by a procedure similar to that described by Sudmeier et al. (1981). The hybrid species all exhibited Co^{3+} spectral bands in the UV–visible range (300–800 nm) indistinguishable from the Co^{3+} bands of the $(In)_6(Co^{3+})_2$ hexamer (Figure 1B).

Results and Discussion

Preparation and Characterization of Cd^{2+}, Co^{2+}, and Co^{3+}-Substituted Insulins. Our Sephadex G-100 column chromatography shows substitution of Cd^{2+}, Co^{2+}, and Co^{3+} for Zn^{2+} gives high yields of insulin hexamers. In agreement with our ^{113}Cd NMR work (Sudmeier et al., 1981), at relatively high insulin and Cd^{2+} concentrations substitution of Cd^{2+} results in the formation of a stable $(In)_6(Cd^{2+})_2Cd^{2+}$ species, whereas substitution of Co^{2+} and oxidation of the insulin-bound Co^{2+} to Co^{3+} results in the formation respectively of stable $(In)_6(Co^{2+})_2$ and $(In)_6(Co^{3+})_2$ species.[2] By comparison with the elution profiles of the native zinc–insulin hexamer and appropriate molecular weight standards (Dunn et al., 1980), the majority of each insulin sample eluted with an apparent M_r of 36 000 ± 4000. As determined by the amino acid analyses in Table I, substitution of Co^{2+} and oxidation to Co^{3+} does not alter the amino acid content of insulin. The visible

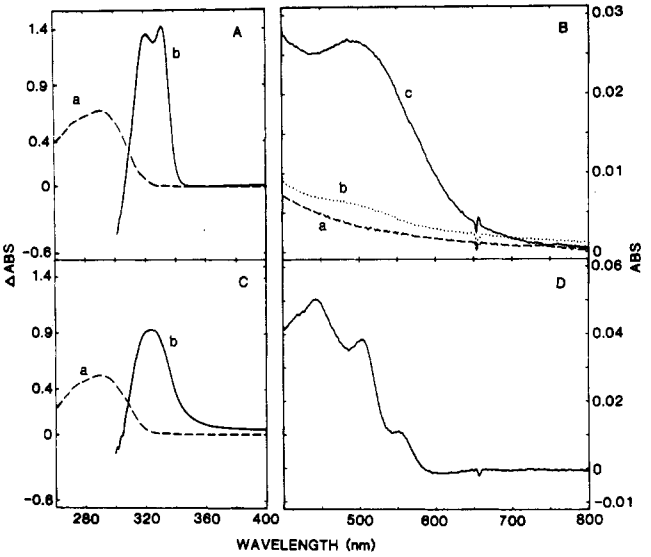

FIGURE 1: Comparison of UV–visible spectra and difference spectra for 47.9 μM terpy (A, trace a, and C, trace a), the bis(terpy)–Cd^{2+} complex (A, trace b), metal-free porcine insulin (B, trace a), $(In)_6(Co^{2+})_2$ (B, trace b), $(In)_6(Co^{3+})Cd^{2+}$ (B, trace c), and the $(terpy)_2Co^{3+}$ complex (C, trace b, and D). The spectra in A (trace a) and B (trace a) are for 42.9 and 32.8 μM terpy, respectively. The difference spectra in A, C, and D (—) subtract the spectrum of a 0.174 mM terpy reference solution from a sample solution containing 0.174 mM terpy and either 42.9 μM Cd^{2+} (A, trace b) or 32.8 μM Co^{3+} (C, trace b, and D). The spectra in (B) are (a) 0.144 mM porcine In (monomer), (b) plus 61.5 μM $Co(OAc)_2$ and 30.7 μM $Cd(NO_3)_2$, and (c) after incubation for 90 min with 67.7 mM H_2O_2. All spectra were measured in 50 mM Tris–$HClO_4$ buffer, pH 8.0, at 25 °C.

spectra (400–800 nm) for $(In)_6(Co^{2+})_2$ and $(In)_6(Co^{3+})_2$ are shown in Figure 1B. In agreement with the coordination found for zinc ion bound to the His(B10) sites in crystalline $(In)_6(Zn^{2+})_2$ (Blundell et al., 1972), the energies and extinction coefficients of the d–d transitions in the visible spectra (Figure 1B) indicate that both Co^{2+} and Co^{3+} reside in a highly symmetric octahedral ligand field[2] (Cotton & Wilkinson, 1972; Urdea & Legg, 1979).

Amino Acid and Peptide Analyses of $(In)_6(^{57}Co^{2+})_2$ and $In_6(^{57}Co^{3+})_2$. The data presented in Table I demonstrate that the incorporation of $^{57}Co^{2+}$ into bovine $(In)_6(^{57}Co^{2+})_2$ and the oxidation of $(In)_6(^{57}Co^{2})_2$ to $(In)_6(^{57}Co^{3+})_2$ do not alter the amino acid analysis. The amino acid composition of $^{57}Co^{3+}$-labeled B chains generated via the oxidation of the

[2] Preliminary X-ray diffraction studies of rhombodhedral porcine $(In)_6(Co^{3+})_2$ crystals show that this derivative is isomorphous with rhombohedral porcine $(In)_6(Zn^{2+})_2$ and that intensity differences between the diffraction patterns of the two derivatives are minor (F. Coffman, G. Dodson, and M. F. Dunn, unpublished results).

Table II: Amino Acid Analysis of ^{57}Co-Labeled Insulin B Chains and of the Purified ^{57}Co-Labeled Peptide from the Thermolysin Digest

amino acid	^{57}Co(III)-labeled insulin B chain: yield[a]	^{57}Co(III)-labeled insulin B chain: residues[b]	insulin B chain expected[c]	^{57}Co(III) yield of amino acid (nmol)	labeled peptide from no. of residues found (relative to His)	thermolytic digest[e,f]
Lys	5.8	1.1	1			
His	10.6	2.0	2	12.7	1.0	1.0
Arg	4.8	0.9	1	0.9	0.1	
cysteic acid	9.5	1.8	2	11.2	0.9	1.0
Asp	6.4	1.2	1	0.6	0.05	
Thr	4.7	0.9	1			
Ser	4.2	0.8	1	8.6	0.7[d]	1.0
Glu	18.0	3.4	3	2.0	0.2	
Pro	5.7	1.1	1			
Gly	16.4	3.1	3	12.7	1.0	1.0
Ala	11.7	2.2	2			
$^1/_2$-Cys						
Val	14.3	2.7	3	1.7	0.1	
Met						
Ile						
Leu	20.7	3.9	4	10.3	0.8[d]	1.0
Tyr	9.0	1.7	2			
Phe	14.8	2.8	3	1.6	0.1	

[a] Nanomoles. [b] Relative to His as 2. [c] On the basis of the insulin B chain sequence and performic acid oxidation. [d] Uncorrected for degradation losses. [e] Note that the composition data do not distinguish between the peptides Leu(B6)-Cys(B7)-Gly(B8)-Ser(B9)-His(B10) and His(B5)-Leu-(B6)-Cys(B7)-Gly(B8)-Ser(B9). However, only the former peptide is expected to be generated by cleavage with thermolysin. [f] Theoretically expected number of residues for the peptide Leu(B6)-Cys(B7)-Gly(B8)-Ser(B9)-His(B10). Relative to His as 2.

interconnecting disulfide linkages by performic acid is also unchanged (Table II).

Three ^{57}Co-labeled peptides were isolated from the digestion of the B chains with thermolysin. The major peptide isolated (representing 56% of the ^{57}Co present) was found to have a composition (Table II) corresponding to the sequence Leu-(B6)-Cys(B7)-Gly(B8)-Ser(B9)-His(B10). However, due to the presence of a second histidyl residue at position B5, the composition of this peptide is not unique, and a priori the peptide could have the sequence His(B5)-Leu(B6)-Cys-(B7)-Gly(B8)-Ser(B9). A single cycle of Edman degradation of the peptide resulted in the positive identification of leucine as the N-terminal amino acid. Consequently, these data indicate that in solution Co^{3+}, and by inference Co^{2+}, occupies the His(B10) sites[2] in $(In)_6(^{57}Co^{3+})_2$ and $(In)_6(^{57}Co^{2+})_2$.

Kinetics of Terpy Reactions with the Exchange-Labile Co^{2+} and Cd^{2+} Hexamers. As documented above, stable $(In)_6(Cd^{2+})_2Cd^{2+}$ hexamers can be prepared when In and Cd^{2+} at high concentrations are mixed in a ratio of 3:1. To compare the kinetics of the reaction of terpy with Co^{2+} and Cd^{2+} bound to the His(B10) sites, experimental conditions (viz., Figure 2) were chosen to minimize metal ion binding to the Glu(B13) site. Therefore, kinetic studies were carried out with ratios of [metal ion] to [In] = 0.064. Since both Co^{2+} and Cd^{2+} bind more tightly to the His(B10) sites, a large excess of insulin over metal ion favors binding to these sites.[2] The kinetic time courses observed for the sequestering and removal of Cd^{2+} and Co^{2+} by terpy from the corresponding insulin hexamers (Figure 2) are strikingly similar to the time courses reported by Dunn et al. (1980) for the Zn^{2+} system. With all three metal ions, the reactions are biphasic. In each instance, the rate observed in the fast phase was found to be proportional to the concentration of terpy, whereas the rate of the slow phase saturates at high terpy, and the amplitude of the fast phase saturates at a value equal to 40–80% of the total change. The saturated slow-phase rate constants are nearly identical for all three metal ions ($0.6 \pm 0.1\ s^{-1}$), and the apparent second-order rate constants for the fast phase are similar ($1 \times 10^4\ M^{-1}\ s^{-1}$ to $4 \times 10^4\ M^{-1}\ s^{-1}$). These second-order rate constants are much too slow to be limited by the loss of inner sphere coordinated water molecules (Eigen & Wilkins, 1964; Holyer et al., 1966;

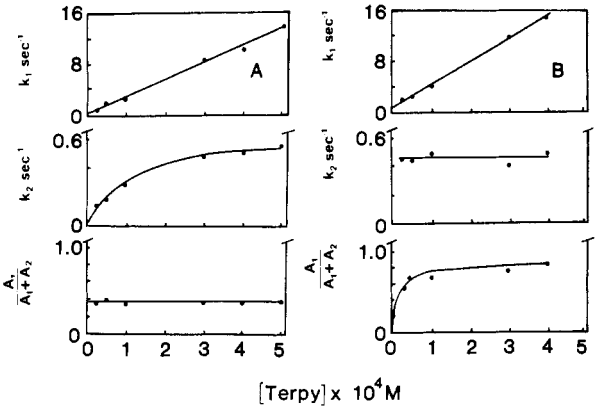

FIGURE 2: Dependence of rates and relative amplitudes of the biphasic 330-nm time courses observed in the reactions of terpy with bovine $(In)_6(Co^{2+})_2$ [shown in (A)] and bovine $(In)_6(Cd^{2+})_3$ [shown in (B)]. See Methods for details of the experiment. Final concentrations after mixing were [terpy] = 500 μM, [In] (monomers) = 75 μM, and [metal ion] = 4.8 μM, all were in pH 8.0 Tris-HCl buffer (0.05 M), 25.0 ± 5 °C.

Dunn, 1975). When higher [metal ion] to [In] ratios are employed (i.e., $\simeq$0.33 for Co^{2+} or $\simeq$0.50 for Cd^{2+}), the observed time courses were found to be similar (data not shown). As previously proposed for the zinc–insulin hexamer (Dunn et al., 1980), the kinetic behavior of the terpy reaction is consistent with a mechanism involving a rapid initial step in which a terpy molecule coordinates to each His(B10)-bound metal ion via displacement of the three water molecules from the octahedral ligand field. In the slow phase, the terpy-coordinated metal ion then dissociates from the protein (P) and a second molecule of terpy is coordinated by the metal ion, forming a bis(terpy) complex:

$$\text{terpy} + (H_2O)_3M^{2+}(P) \overset{\text{fast}}{\rightleftharpoons} (\text{terpy})M^{2+}(P) + 3H_2O \quad (1)$$

$$(\text{terpy})M^{2+}(P) \overset{\text{slow}}{\rightleftharpoons} (\text{terpy})M^{2+} + P \quad (2)$$

$$(\text{terpy})M^{2+} + \text{terpy} \xrightarrow{\text{fast}} (\text{terpy})_2M^{2+} \quad (3)$$

This kinetic behavior very clearly has its origins both in the structure of the ligand field about the metal ion and in the

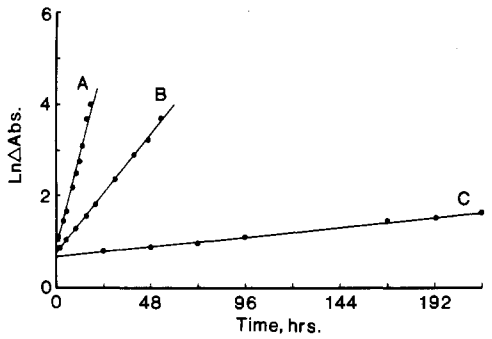

FIGURE 3: Stability of bovine $(In)_6(Co^{3+})_2$ determined by reaction with excess terpy. The rate of the reaction of terpy with the Co^{3+}-insulin hexamer was determined under three sets of conditions. The time courses were found to be adequately described as pseudo-first-order processes. The half-life for the release of cobalt from Co^{3+}-insulin in buffer at pH 8.0 was found to be 13.1 h (B). Under identical conditions, but with the addition of 1 mM potassium ferrous cyanide, the half-life is reduced to 4.4 h (A). Conversely, in the presence of 1 mM H_2O_2, the half-life is increased to 148 h.

structure of the obligate planar tridentate chelator. For example, when the structure of the ligand field about the metal ion is different (i.e., tetrahedral or pentacoordinate with only a single inner sphere coordinated water molecule, viz., the active site zinc ions of liver alchol dehydrogenase or carboxypeptidase), reaction with terpy is very slow and monophasic (Dunn et al., 1980).

Kinetics of Terpy Reactions with Exchange-Inert Co^{3+} Hexamers and with Hybrid Co^{3+}–Cd^{2+} Hexamers. In Figure 1, the spectrum of terpy (A, trace a), the difference spectra comparing the bis(terpy)–Cd^{2+} complex (A, trace b) and the bis(terpy)–Co^{3+} complex (C, trace b, and D) to terpy, and the spectra of $(In)_6(Co^{2+})_2$ and $(In)_6(Co^{3+})_2$ (B, traces b and c) are shown for comparison. Formation of the bis complexes with Cd^{2+} and Co^{3+} causes the spectrum of the terpy chromophore to shift to longer wavelengths, and the bis complexes are characterized by large extinction coefficient changes $\Delta\epsilon^{Cd}_{332} = 3.32 \times 10^4\ M^{-1}\ cm^{-1}$, $\Delta\epsilon^{Co}_{320} = 2.88 \times 10^4\ M^{-1}\ cm^{-1}$). The $(terpy)_2Co^{3+}$ complex also exhibits characteristic d–d transitions in the 400–800-nm region with peak absorbances occurring at 440, 503, and 550 nm (Figure 1D), whereas the $(In)_6(Co^{3+})_2$ complex exhibits a broad band centered at 488 nm (Figure 1B, trace c). Consequently, the spectral changes that occur upon the sequestering and removal of insulin-bound Cd^{2+} and/or Co^{3+} by terpy provide a convenient means both for following the kinetics of these processes and for characterizing the products.

In contrast to the kinetic lability exhibited by the Zn^{2+}, Cd^{2+}, and Co^{2+} hexamers, the Co^{3+} species (as anticipated) is kinetically inert; the sequestering and removal of Co^{3+} by terpy occurs on a time scale of hours to days (Figure 3). The kinetics of this reaction are adequately described by a first-order rate law. The half-time for the release of cobalt from $(In)_6(Co^{3+})_2$ at pH 8.0 was found to be 13.1 h. This can be compared to a half-time of 4.4 h for a sample of $(In)_6(Co^{3+})_2$ incubated under identical conditions but in the presence of the reducing agent 1 mM potassium ferrocyanide. Conversely, in the presence of a mild oxidizing agent, 0.1 mM H_2O_2, a half-time of 148 h was found. These data confirm small molecule studies showing that the mechanism of ligand exchange for Co^{3+} complexes (Cotton & Wilkinson, 1972) involves exchange of a single electron with reduction to Co^{2+}.

Consequently, it can be concluded that the predominant pathway for ligand substitution in the $(In)_6(Co^{3+})_2$ complex occurs via the intermediacy of the exchange-labile Co^{2+} complex (eq 4–6) and that conversion of Co^{3+} to Co^{2+} (eq 4) limits

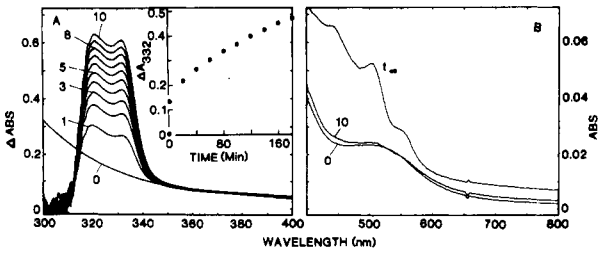

FIGURE 4: (A) Time-resolved UV–visible difference spectra for the reaction of terpy with porcine $(In)_6(Co^{3+})_2Cd^{2+}$ in 50 mM Tris-$HClO_4$ buffer, pH 8.0, at 25 °C. Reaction was initiated by introducing equal concentrations of terpy into a reference cuvette containing buffer and a sample cuvette containing the hybrid hexamer. Scanning was initiated immediately upon completion of mixing with 20-min intervals between scans 1–10 and approximately 13–15 s between scan 0 and scan 1. Scan 0 is the spectrum of the hybrid just prior to the addition of terpy. The inset to (A) shows the time course for the absorbance changes measured at 332 nm. The traces in (B) show the Co^{3+} d–d bands just prior to the addition of terpy (scan 0), after 180 m (scan 10) and at 36 h (t_∞). The hybrid hexamer was prepared as described under Materials and Methods by incubating In, Co^{2+}, Cd^{2+}, and H_2O_2 for 4.5 days prior to the addition of terpy. [In] (monomers) = 0.178 mM; [cobaltus acetate] = 60.2 μM; [$Cd(NO_3)_2$] = 15.1 μM; [H_2O_2] = 66.5 mM; [terpy] = 99 μM. Conditions giving a [In]:[Co^{2+}]:[Cd^{2+}] ratio of 6:2:0.5 were chosen to ensure an excess of hexamer sites over Cd^{2+}.

the rate of terpy reaction in the $(In)_6(Co^{3+})_2$ system. Because reduction of Co^{3+} to Co^{2+} is the slow step, appearance of the bis complex is a pseudo-first-order process:

$$Co^{3+}(P) + e^- \underset{}{\overset{\text{slow}}{\rightleftharpoons}} Co^{2+}(P) \quad (4)$$

$$Co^{2+}(P) + 2terpy \xrightarrow{\text{fast}} P + (terpy)_2Co^{2+} \quad (5)$$

$$(terpy)_2Co^{2+} \xrightarrow{\text{fast}} (terpy)_2Co^{3+} + e^- \quad (6)$$

To explore the metal binding properties of the Glu(B13) site, hybrid hexamers containing His(B10) sites substituted with Co^{3+} and the Glu(B13) site substituted with Cd^{2+} were prepared and the reactions of this hybrid hexamer with terpy were studied by UV–visible spectroscopy. The time-resolved UV–visible spectral changes (300–600 nm) that occur when terpy is mixed with the $(In)_6(Co^{3+})_2Cd^{2+}$ hybrid are shown in Figure 4. The time course consists of a burst phase that is complete within the mixing deadtime (13–15 s), a slow phase with a $t_{1/2} \simeq 1$ h, and a third, very slow phase (not shown) that occurs on a time scale of days. Comparison of the spectral changes that take place in these three phases with the spectra presented in Figure 1 establishes that each of the first two phases are dominated by the formation of the bis(terpy)–Cd^{2+} complex, while the third phase involves the formation of the bis(terpy)–Co^{3+} complex. During the first two phases, the appearance of the spectral bands at 320 and 330 nm indicates almost all of the Cd^{2+} present is converted to the $(terpy)_2Cd^{2+}$ complex ($\sim$80% in the first 180 min), while there is almost no change in the 488-nm spectral band that characterizes coordination of Co^{3+} to the His(B10) sites (compare Figures 1B, trace c, and 4B, traces 0 and 10). However, during the third phase, this region of the spectrum undergoes a conversion to the spectrum of the $(terpy)_2Co^{3+}$ complex (compare the t_∞ trace of Figure 4B with Figure 1D).

When Cd^{2+} is added to a preformed $(In)_6(Co^{3+})_2$ hexamer (with Cd^{2+} added in the amount of $\leq$1 mol per hexamer and with all initial concentrations the same as in Figure 4), followed by the immediate addition of excess terpy (within 1 min of the addition of Cd^{2+}), there occurs a fast burst reaction that is complete within the mixing deadtime (13–15 s). The amplitude of this burst reaction (data not shown) and the resulting

spectral bands indicate that all of the Cd^{2+} present is converted to the $(terpy)_2Cd^{2+}$ complex. When the Cd^{2+} added is incubated with the $(In)_6(Co^{3+})_2$ hexamer preparation for 4 h prior to the addition of terpy, almost all (90%) of the total Cd^{2+} is converted to the $(terpy)_2Cd^{2+}$ complex in a fast burst reaction.

The two phases detected in the reaction of terpy with the hybrid hexamer (Figure 4), strongly imply the presence of two classes of Cd^{2+}. The fast phase of the reaction occurs within 13–15 s and, therefore, appears to involve either the aquated Cd^{2+} ion or Cd^{2+} which is weakly bound to the outside surface of the hexamer. Certainly, there is no high activation energy to the sequestering of Cd^{2+} in this phase. The second phase occurs on a time scale of hours, and thus *must represent an insulin-bound Cd^{2+} species that only releases Cd^{2+} slowly.* Two pieces of evidence identify the site involved as a site with only moderate affinity for Cd^{2+}: (1) Even though the hexamer concentration used in these experiments significantly exceeds a stoichiometry of one hexamer per Cd^{2+} ion added, a significant fraction of the total Cd^{2+} reacts in the fast phase. (Variation of incubation times from 2 h to 4 days indicates that equilibrium is achieved during the oxidation step of the hybrid preparation.) Calculations based on the amounts of fast and slowly reacting Cd^{2+} measured in experimnts similar to that reported in Figure 4 for varying ratios of $[Cd^{2+}]$/[hexamer] give an estimated Cd^{2+} dissociation constant, $K_D^{Cd} \simeq 4 \pm 2$ μM. (2) A 3–4-fold excess of terpy provides a thermodynamic drive that is sufficient to convert all the Cd^{2+} to the $(terpy)_2Cd^{2+}$ complex. When taken together with the NMR studies of Sudmeier et al. (1981), these findings strongly suggest that because of the exchange-inert properties of Co^{3+}, the $(In)_6(Co^{3+})_2$ hexamer is a cage that sequesters Cd^{2+} (or Ca^{2+}, see below) at the center of the hexamer in a ligand field provided by the side chain carboxylate moieties of the Glu(B13) residues (viz., Chart I). Due to the exchange-inert kinetic properties of the Co^{3+} ions substituted into the His(B10) sites,[2] the $(In)_6(Co^{3+})_2$ hexamer is a kinetically stable species; and relative to the $(In)_6(Zn^{2+})_2$ and $(In)_6(Cd^{2+})_2Cd^{2+}$ species, both subunit dissociation and Co^{3+} exchange undoubtedly are slow processes.

Calcium Binding to Insulin. The above-described experiments and the results of the ^{113}Cd NMR spectroscopy study of insulin (Sudmeier et al., 1981) indicate that the hexamer has an internal metal binding site involving the Glu(B13) carboxylates (Chart I) and that this site appears to be specific for Ca^{2+} and Cd^{2+}. In an effort to further define this binding site, equilibirum dialysis was used to study the binding of $^{45}Ca^{2+}$ to the two-zinc insulin hexamer and to metal-free insulin.

Figure 5A shows the results of $^{45}Ca^{2+}$ binding to the two-zinc insulin hexamer at a concentration of 0.29 mM hexamer (i.e., 1.74 mM insulin monomer). The straight line is drawn through the data points in this Scatchard plot by a linear least-squares analysis program. The inset to the diagram shows the data plotted as a binding isotherm. The hyperbolic line was computer generated from the noncooperative binding equation

$$v = nL_f/(K_d + L_f) \quad (7)$$

with the dissociation constant, K_d, and number of binding sites, n, obtained from Scatchard analysis. It appears that these data are adequately fit by assuming a single Ca^{2+} binding site (i.e., $n = 0.98 \pm 0.05$) with a K_d of 83 μM. However, the existence of weaker binding sites for Ca^{2+} is not excluded.

Figure 5B shows the results of $^{45}Ca^{2+}$ binding to an otherwise metal-free insulin sample at the same concentration (i.e., 1.74 mM insulin monomers, 0.29 mM potential hexamers). By use of the same analytical criteria, these data appear to be adequately fit by assuming one site per dimer (or three sites per putative hexamer) with an apparent mean dissociation constant of 1.7 mM.

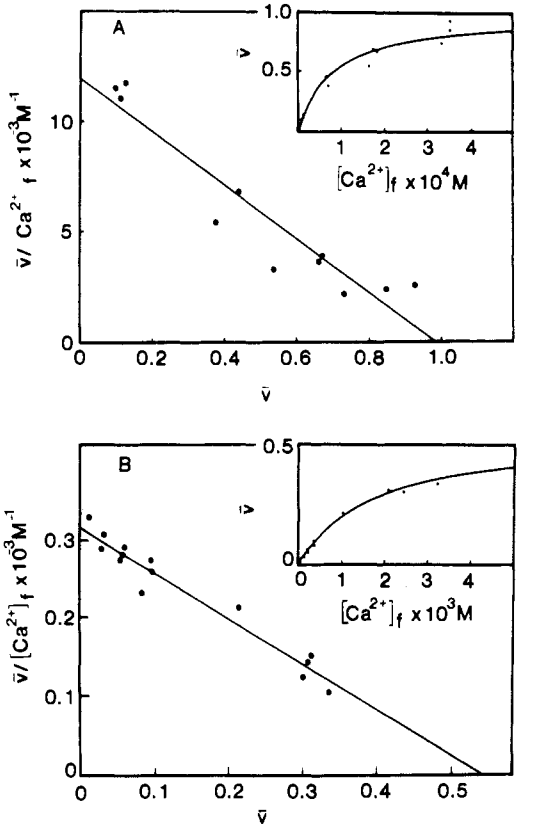

FIGURE 5: Scatchard plots of $^{45}Ca^{2+}$ binding to the two zinc–insulin hexamer (A) and to metal-free insulin (B). (A) The hexamer concentration is 290 μM (i.e., 1.74 mM insulin monomer) to which has been added 580 μM Zn^{2+}. The straight line has been drawn as the best fit to a linear least-squares analysis program. The insert to the figure shows the individual data plotted as a binding isotherm, and the hyperbolic line drawn through the data has been computer generated from a noncooperative binding equation, $v = nL_f/(K_d + L_f)$, for dissociation constant $K_d = 83$ μM with the number of binding sites $n = 0.98$ (values obtained from the Scathchard analysis). (B) The insulin (monomer) concentration is 1.75 mM. Data were analyzed as in (A) yielding a dissociation constant $K_d = 1.7$ mM and the number of binding sites $n = 0.53$.

Although Cd^{2+} is an exchange-labile metal ion (viz., Figure 2), the kinetic experiments reported in this paper indicate that there is a significant energy barrier to the dissociation of Cd^{2+} from the Glu(B13) site of the hybrid hexamer even though this site appears to bind Cd^{2+} with only moderate affinity ($K_D = 4 \pm 2$ μM). Examination of the three-dimensional structure of the zinc–insulin hexamer (Blundell et al., 1972; viz., Chart I) indicates that one obvious route of escape from the Glu(B13) site of an intact hexamer lies along the solvent filled channel along the hexamer 3-fold symmetry axis. With the His(B10) sites occupied by Co^{3+} ions,[2] it is likely that large potential energy barriers exist at either end of the hexamer that would impede the diffusion of Cd^{2+} along the channel. The His(B10)-bound Co^{3+} ions undoubtedly contribute Coulombic force fields that would oppose the close approach of Cd^{2+}. Alternatively, the dimensions of the channel could retard the rate of diffusion of Cd^{2+}. Any constrictions in the channel could limit the rate of diffusion of the aquated Cd^{2+} ion, thus providing a van der Waals barrier and/or an electrostatic barrier to the escape of Cd^{2+}. Indeed, the rate of Cd^{2+} escape

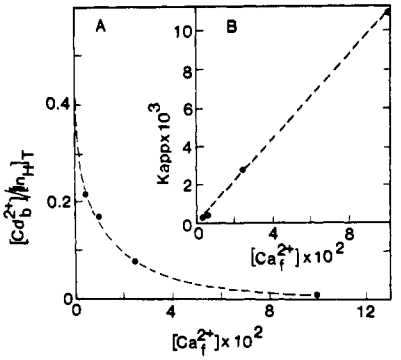

FIGURE 6: Effects of Ca^{2+} on the amount of Cd^{2+} bound to the Glu(B13) sites. (A) The dependence of $[Cd^{2+}_f]/[In_H]_T$ on $[Ca^{2+}]$. The amounts of bound calcium, Cd^{2+}_b, were estimated from measurements of the amplitude of the fast phase of the terpy reaction (viz., Figure 4) as a function of the concentration of Ca^{2+} present. Values of K_{app} then were calculated from eq 10 for each data point in (A), and these values were used to construct the plot of K_{app} vs. $[Ca^{2+}_f]$ shown in (B). According to eq 11, the plot in (B) gives an intercept = K_D^{Cd} and a slope = K_D^{Cd}/K_D^{Ca}. The intercept is too small to be accurately determined. Assuming a value of $K_D^{Cd} = 4$ μM (see text), the slope yields a value for $K_D^{Ca} \sim 40$ μM. The data were obtained from experiments run under conditions similar to those used in Figure 4 but with Ca^{2+} added before oxidation with H_2O_2.

could be limited by channel dimensions that require partial desolvation of Cd^{2+}.

Since the rate of escape of Cd^{2+} is faster than the rate of terpy reaction with Co^{3+} bound to the His(B10) sites, the reaction of terpy in the second phase is not due to the breakdown of hexamers by the sequestering and removal of Co^{3+}. However, the reversible dissociation of the hybrid to an $(In)_3Co^{3+}$ trimer with the release of Cd^{2+} cannot be ruled out as a possible pathway for the reaction:

$$(In)_6(Co^{3+})_2Cd^{2+} \underset{\text{slow}}{\rightleftharpoons} 2(In)_3Co^{3+} + Cd^{2+} \quad (8)$$

$$Cd^{2+} + 2\text{terpy} \rightarrow (\text{terpy})_2Cd^{2+} \quad (9)$$

Competition between Cd^{2+} and Ca^{2+} for the Glu(B13) Site. To investigate the influence of Ca^{2+} on the binding of Cd^{2+} to the Glu(B13) site of $(In)_6(Co^{3+})_2$ hexamers, Ca^{2+} was incubated with insulin along with Co^{2+} and Cd^{2+} prior to the oxidation of Co^{2+} to Co^{3+} with H_2O_2. The resulting hexamer preparations were then assayed via the terpy reaction to determine the proportion of fast and slow reacting Cd^{2+} as a function of the initial Ca^{2+} concentration. Under conditions where the concentrations of insulin, Co^{3+}, and Cd^{2+} are held constant (with a ratio of 6:2:1) and the concentration of Ca^{2+} is varied, it was found that the proportion of reaction occurring in the burst phase increases when the concentration of Ca^{2+} is increased (Figure 6). At high Ca^{2+} concentration (10 mM) almost all of the Cd^{2+} present was found to react in the burst phase. The hyperbolic dependence evident in Figure 6 is indicative of a competition between Cd^{2+} and Ca^{2+} for a single class of binding sites. Since Ca^{2+} does not compete with Zn^{2+} for the His(B10) sites (Sudmeier et al., 1981), it is unlikely that the competition between Cd^{2+} and Ca^{2+} involves the His(B10) sites. The ^{113}Cd NMR studies of Sudmeier et al. (1981) indicate that addition of Ca^{2+} to the $(In)_6(Cd^{2+})_2Cd^{2+}$ hexamer results in the displacement of Cd^{2+} from the Glu(B13) site but not from the His(B10) sites, and the results presented in Figure 6 are consistent with this interpretation. The solid line in Figure 6 is the best fit of the data to the hyperbolic equation for a strictly competitive binding model involving a single class of noninteracting sites (eq 10), where the subscripts f, b, and T designate free, bound, and total concentrations, $[In_H]_T$ is the total hexamer concentration, and

$$[Cd^{2+}_b]/[In_H]_T = \frac{[Cd^{2+}_f]}{K_D^{Cd}(1 + [Ca^{2+}_f]/K_D^{Ca}) + [Cd^{2+}_f]} = \frac{[Cd^{2+}_f]}{K_{app} + [Cd^{2+}_f]} \quad (10)$$

K_D^{Ca} and K_D^{Cd} are the calcium and cadmium dissociation constants. When analyzed according to eq 11, the data give

$$K_{app} = K_D^{Cd} + [Ca^{2+}_f](K_D^{Cd}/K_D^{Ca}) \quad (11)$$

an estimate of $K_D^{Ca} \simeq 40$ μM (calculated from the slope of the straight line drawn through the data points in the inset to Figure 6 with the assumption that $K_D^{Cd} = 4$ μM). This estimate is in reasonable agreement with the value of 83 μM obtained for the $(In)_6(Zn^{2+})_2Ca^{2+}$ system (Figure 5A).

Blundell et al. (1972) reported that substitution of Cd^{2+} for Zn^{2+} results in crystalline hexamers containing 3 mol of Cd^{2+} per hexamer; two of the cadmium ions reside in the His(B10) sites; the third is located in the vicinity of the Glu(B13) carboxylates at the center of the hexamer. Heavy metal replacement studies showed occupancy of the Glu(B13) site by Pb^{2+} and UO_2^{2+} (Blundell et al., 1972; Adams et al., 1969; Hodgkin et al., 1972). More recently, Emdin et al. (1980) reported that crystalline rhombohedral insulin hexamers containing 5 mol of Zn^{2+} per hexamer can be prepared. In this structure, two of the zincs occupy the His(B10) sites, the remaining three are symmetrically arranged about the 3-fold symmetry axis at the center of the hexamer, each coordinated to a pair of Glu(B13) carboxylates:

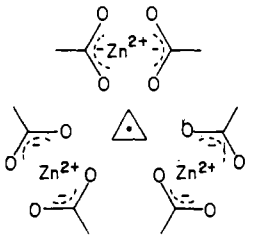

Our preliminary ^{113}Cd NMR studies (Sudmeier et al., 1981) and data reported herein indicate a single Cd^{2+} or Ca^{2+} binds with high affinity to the Glu(B13) site. Thus far, attempts to clearly demonstrate additional, weaker binding sites have been inconclusive. If the binding of metal ions to the central cavity defined by the Glu(B13) carboxylates is negatively cooperative (a not unexpected happenstance), then the differences in stoichiometry [one Ca^{2+} site detected in these experiments vs. three Zn^{2+} sites detected by Emdin et al. (1980)] may simply be a consequence of the experimental conditions used. The studies of Emdin et al. (1980) involve effective concentrations of 10–100 mM for both insulin and metal ion in the crystalline state. In our experiments, any negative cooperativity involving apparent K_D values > 5 mM would be difficult to detect. Consequently, our relatively dilute conditions (≤0.5 mM) favor detection of high-affinity sites, while rendering detection of weaker sites more difficult.

As shown by the data in Figure 5B, zinc-free insulin also binds calcium ion but with lower affinity ($K_D \simeq 1$ mM at 4 °C). The abscissa intercept indicates a stoichiometry of one site per dimer or three sites per putative hexamer. Attempts to demonstrate a calcium–insulin hexamer via Sephadex G-100 chromatography failed, indicating that either such a hexamer is too unstable to survive gel filtration or that the calcium binding species is the insulin dimer. Although the protein residues involved in coordination of calcium to zinc-free (probably dimeric) insulin are not known, the Glu(B13) residues are likely candidates.

The relationship of the Glu(B13) calcium binding sites in hexameric insulin to the biological function is unknown. Since Ca^{2+} binds less tightly to zinc-free insulin by more than 1 order of magnitude, Ca^{2+} binding must favor the hexamer over dimer. Since at the level of hormone–receptor interaction the biologically functional form of insulin is the monomer, the complex set of equilibria involved in the formation of monomer from hexamer may be an important component of the mechanism by which monomeric insulin levels are regulated. These studies indicate that the highly cooperative assembly of $(In)_6(Zn^{2+})_2$ is further modulated by calcium binding. The reports indicating that insulin storage granules contain high concentrations of Ca^{2+} (Howell et al., 1975) suggest to us that insulin is stored in the form of a quasi-crystalline array of hexamers (Greider et al., 1969) with the His(B10) sites occupied by zinc and the Glu(B13) site(s) occupied by calcium. Both solution evidence and crystallographic evidence for additional divalent metal ion binding sites on the surface of the hexamer suggest that additional sites may also be filled by zinc and calcium.

ACKNOWLEDGMENTS

We thank Gerald Porter (Biochemistry Department, University of California, Riverside, CA) for performing the peptide N-terminal analysis and J. L. Evelhoch (Chemistry Department, University of California, Riverside, CA) for performing some of the atomic absorption spectroscopy. We also thank Professor Anthony Norman (Biochemistry Department, University of California, Riverside, CA) for his gift of $^{45}Ca^{2+}$.

Registry No. Terpy, 1148-79-4; Ca, 7440-70-2; Cd, 7440-43-9.

REFERENCES

Adams, M. J., Blundell, T. L., Dodson, E. J., Dodson, G. G., Vijayan, M., Baker, E. N., Harding, M. M., Hodgkin, D. C., Rimmer, B., & Sheat, S. (1969) *Nature (London) 224*, 491–495.

Blundell, T., Dodson, G. G., Hodgkin, D., & Mercola, D. (1972) *Adv. Protein Chem. 26*, 279–402.

Brill, A. S., & Venable, J. H. (1967) *J. Am. Chem. Soc. 89*, 3622–3626.

Brill, A. S., & Venable, J. H. (1968) *J. Mol. Biol. 36*, 343–353.

Cotton, F. A., & Wilkinson, G. (1972) in *Advanced Inorganic Chemistry*, 3rd ed., p 885, Wiley-Interscience, New York.

Dunn, M. F. (1975) *Struct. Bonding (Berlin) 23*, 61–122.

Dunn, M. F., Bernhard, S. A., Anderson, D., Copeland, A., Morris, R. G., & Rogue, J.-P. (1979) *Biochemistry 18*, 2346–2354.

Dunn, M. F., Pattison, S. E., Storm, M. C., & Quiel, E. (1980) *Biochemistry 19*, 718–725.

Eigen, M., & Wilkins, R. G. (1964) in *Mechanisms of Inorganic Reactions* (Gould, R. F., Ed.) pp 55–80, American Chemical Society, Washington, DC.

Emdin, S. O., Dodson, G. G., Cutfield, J. M., & Cutfield, S. M. (1980) *Diabetologia 19*, 174–182.

Fredericq, E. (1954) *J. Polym. Sci. 12*, 287–300.

Furlong, C. E., Morris, R. G., Kandrach, M., & Rosen, B. P. (1972) *Anal. Biochem. 47*, 514–526.

Greider, M. H., Howell, S. L., & Lacy, P. E. (1969) *J. Cell Biol. 41*, 162–166.

Hirs, C. H. W. (1967) *Methods Enzymol. 11*, 197–199.

Hodgkin, D. C., Blundell, T. L., Cutfield, J. F., Cutfield, S. M., Dodson, G. G., Dodson, E. J., Mercola, D. A., & Vijayan, M. (1972) in *Insulin Actions* (Fritz, I. B., Ed.) p 1, Academic Press, New York.

Holyer, R. H., Hubbard, C. D., Kettle, S. F. A., & Wilkins, R. G. (1966) *Inorg. Chem. 5*, 622–625.

Howell, S. L., Montague, W., & Tyhurst, M. (1975) *J. Cell Sci. 19*, 395–409.

Lu, H. S., Yuan, P. M., Talent, J. M., & Gracy, R. W. (1981) *Anal. Biochem. 110*, 159–164.

Moore, S., & Stein, W. H. (1963) *Methods Enzymol. 6*, 819–831.

Pattison, S. E., & Dunn, M. F. (1975) *Biochemistry 14*, 2733–2738.

Spackman, D. H. (1967) *Methods Enzymol. 11*, 3–15.

Spackman, D. H., Stein, W. H., & Moore, S. (1958) *Anal. Chem. 30*, 1190–1206.

Sudmeier, J. L., Bell, S. J., Storm, M. C., & Dunn, M. F. (1981) *Science (Washington, D.C.) 212*, 560–562.

Tanford, C., & Epstein, J. (1954a) *J. Am. Chem. Soc. 76*, 2163–2170.

Tanford, C., & Epstein, J. (1954b) *J. Am. Chem. Soc. 76*, 2170–2175.

Urdea, M. S., & Legg, J. I. (1979) *Biochemistry 18*, 4984–4991.